Limnol. Oceanogr., 59(4), 2014, 1310–1320

doi:10.4319/lo.2014.59.4.1310

Nitric oxide turnover in permeable river sediment

Frank Schreiber,[1,2,3,*] Peter Stief,[1] Marcel M. M. Kuypers,[1] and Dirk de Beer [1]

[1] Max-Planck-Institute for Marine Microbiology, Bremen, Germany
[2] Eawag, Swiss Federal Institute of Aquatic Science and Technology, Department of Environmental Microbiology, Dübendorf, Switzerland
[3] ETH Zurich, Swiss Federal Institute of Technology, Department of Environmental Systems Sciences, Zurich, Switzerland

Abstract

We measured nitric oxide (NO) microprofiles in relation to oxygen (O_2) and all major dissolved N-species (ammonium, nitrate, nitrite, and nitrous oxide [N_2O]) in a permeable, freshwater sediment (River Weser, Germany). NO reaches peak concentrations of 0.13 μmol L^{-1} in the oxic zone and is consumed in the oxic–anoxic transition zone. Apparently, NO is produced by ammonia oxidizers under oxic conditions and consumed by denitrification under microoxic conditions. Experimental percolation of sediment cores with aerated surface water resulted in an initial rate of NO production that was 12 times higher than the net NO production rate in steady state. This initial NO production rate is in the same range as the net ammonia oxidation rate, indicating that NO is transiently the main product of ammonia oxidizers. Stable isotope labeling experiments with the ^{15}N-labeled chemical NO donor S-nitroso-N-acetylpenicillamine (SNAP) (1) confirmed denitrification as the main NO consumption pathway, with N_2O as its major product, (2) showed that denitrification combines one free NO molecule with one NO molecule formed from nitrite to produce N_2O, and (3) suggested that NO inhibits N_2O reduction.

Nitric oxide (NO) is an intermediate and by-product in the N-cycle. NO can be produced by most catabolic pathways involved in the N-cycle, with ammonia oxidizers and denitrifiers mediating the most important production and consumption pathways (Fig. 1; Schreiber et al. 2012). NO is also the precursor of nitrous oxide (N_2O), a potent greenhouse gas and ozone-depleting substance for which formation pathways in nature are under debate. Thus, understanding the biology of NO turnover is a prerequisite to an understanding of the formation pathways for atmospheric N_2O (Schreiber et al. 2012).

A simplified scheme for the N-cycle and the corresponding NO and N_2O formation pathways is shown in Fig. 1. NO is an obligate, catabolic intermediate of (canonical) denitrification produced by nitrite (NO_2^-) reductase (Nir). Then, NO is reduced to N_2O by NO reductase (Nor), and N_2O is further reduced to N_2 by N_2O reductase (Nos; Zumft 1997). Ammonia-oxidizing bacteria (AOB) can produce NO as a by-product via two pathways. Activity of nitrifier-encoded Nir and Nor reduces NO_2^- to NO and N_2O in a pathway termed nitrifier denitrification (Poth and Focht 1985). NO_2^- reduction to NO and further to N_2O in AOB is thought to counteract the accumulation of NO_2^- to toxic concentrations (Beaumont et al. 2004). The difference between nitrifier denitrification and canonical denitrification is the electron donor (ammonium [NH_4^+] vs. organic carbon) and the physiological function (detoxification vs. respiration). In a second, less-well-understood pathway, hydroxylamine oxidoreductase (Hao) oxidizes hydroxylamine (NH_2OH) to NO, which is further reduced to N_2O (Hooper and Terry 1979). Ammonia-oxidizing archaea (AOA) have also been shown to produce N_2O, probably by mechanisms akin to those known from AOB (Santoro et al. 2011). We are not aware of a study that reports on NO production of AOA. However, it has been hypothesized that NO is an intermediate in AOA metabolism (Stahl and de la Torre 2012), because the NO scavenger 2-(4-carboxyphenyl)-4,4,5,5-tetramethylimidazoline-1-oxyl-3-oxide (carboxy-PTIO) inhibits NH_4^+ oxidation by AOA (Shen et al. 2013). In this study, we use the term "ammonia oxidizers" to refer to both AOB and/or AOA, because to date it is not possible to distinguish between NO production by AOB and AOA. In addition, NO_2^--oxidizing bacteria (NOB) have the potential to produce NO via Nir for metabolic regulation (Starkenburg et al. 2008).

Bacteria that perform the dissimilatory reduction of nitrate to NH_4^+ (DNRA) have been shown to produce NO in pure culture from cytochrome *c* NO_2^- reductase (Nrf; Corker and Poole 2003) and nitrate (NO_3^-) reductase (Nar; Gilberthorpe and Poole 2008). Bacteria of the NC10 phylum related to "*Candidatus* Methylomirabilis oxyfera" that mediate the oxygenic nitrite-dependent anaerobic oxidation of methane (N-AOM) and bacteria that perform anaerobic NH_4^+ oxidation (anammox) have been shown to use NO as an intracellular intermediate produced by NO_2^- reductase (Nir; Ettwig et al. 2010; Kartal et al. 2011). Both differ from other N-cycle pathways because NO is not further reduced to N_2O. Rather, N-AOM dismutates NO to form N_2 and O_2, while anammox couples the reduction of NO to a condensation with NH_4^+ to produce hydrazine (N_2H_4).

Moreover, most bacteria (also those not involved in the N-cycle) possess enzymes for NO detoxification. Aerobic NO detoxification is mediated by the oxidation of NO to NO_3^- by the enzyme NO dioxygenase (flavohemoglobins, Hmp; Gardner et al. 1998). Anaerobic detoxification is mediated by the reduction of NO to N_2O by the enzymes flavodiiron NO reductase (flavorubredoxin, NorVW) as well as Hmp (Kim et al. 1999; Gardner et al. 2002).

* Corresponding author: frank.schreiber@eawag.ch

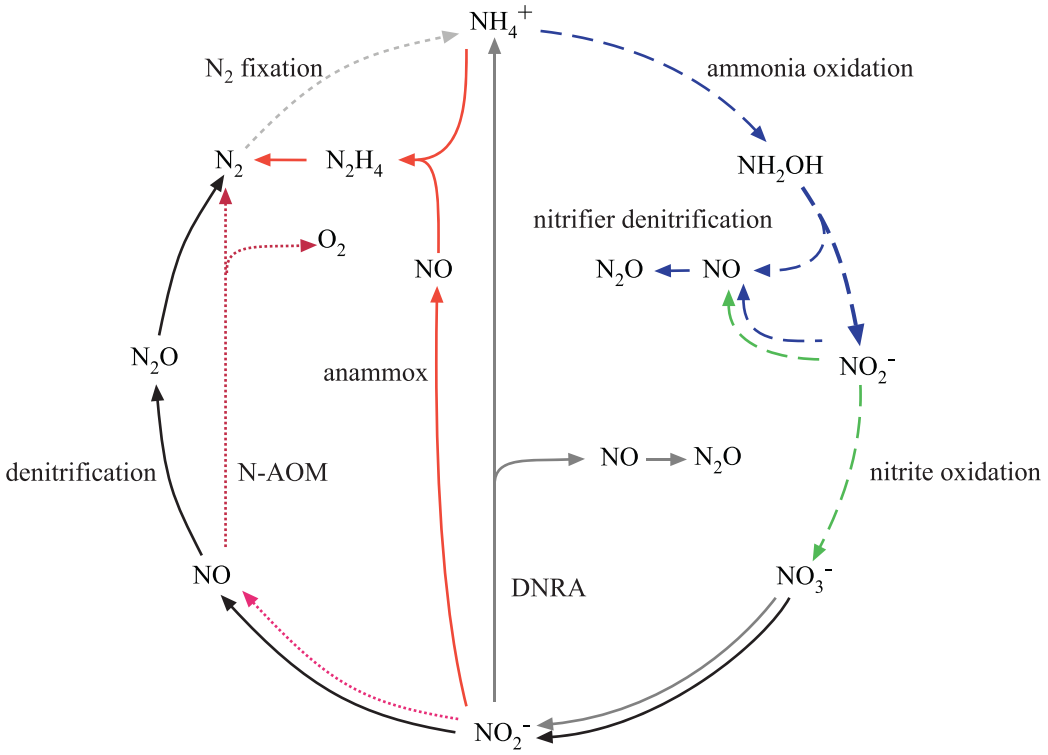

Fig. 1. NO and N_2O formation in N-cycle pathways. DNRA is the dissimilatory NO_3^- reduction to NH_4^+, anammox is the anaerobic oxidation of NH_4^+, and N-AOM is the nitrite-dependent anaerobic oxidation of methane involving the dismutation of NO to O_2 and N_2.

Freshwater streams and rivers have been proposed to be a major source for N_2O to the atmosphere, contributing ~ 10% to the total anthropogenic N_2O emission rate (Beaulieu et al. 2011). N_2O production is thought to mainly take place in the sediments of streams and rivers. Permeable sediments are widespread in streams and rivers, but so far little is known about the mechanisms of N_2O production in these systems. In marine systems, permeable sediments have been shown to promote high turnover rates of inorganic nitrogen (Gao et al. 2010). Thus, permeable freshwater sediments represent relevant sites to investigate the mechanisms of NO turnover to N_2O.

Methodological limitations have so far prohibited research on in situ NO turnover in aquatic sediments in general. Importantly, the sediment strata where NO is produced and how its production is related to the conversion activities of other N-cycle processes (i.e., biogeochemical context) have remained unknown. While N_2O has been studied with microsensors in aquatic sediments (Meyer et al. 2008), only recently did an NO microsensor for measurements in sediments with high spatial resolution (60 μm) and low detection limit (30 nmol L^{-1}) become available (Schreiber et al. 2008).

In the present study, we apply an NO microsensor to permeable river sediment in parallel with other microsensors to elucidate (1) the in situ concentration of NO and (2) the biogeochemical context of NO turnover, and (3) to infer about metabolic pathways that control NO production and consumption. In addition, we conducted stable isotope tracer incubations by introducing ^{15}NO with a ^{15}N-labeled chemical NO donor to study NO consumption pathways.

Methods

Study site and sampling—The study site is located in the Weser River upstream of Bremen, Germany (53.00855°N, 8.98495°E; no tidal influence). The sandy sediment samples (porosity, $\Phi = 0.42$) were retrieved from the riverbank at ~ 30 cm water depth with Perspex core liners. Sampling took place from September to November 2007 (microsensor work) and then again in January 2009 (stable isotope work). The general sediment characteristics, such as porosity, color (brownish, oxidized sediment), and O_2-uptake rate were comparable between these two sampling periods. Also, the dissolved inorganic nitrogen concentrations in the water column were comparable between these two sampling periods (NH_4^+ = 14 μmol L^{-1} and NO_3^- = 190–235 μmol L^{-1}).

Microsensor measurements—Undisturbed sediment cores (diameter = 5.4 cm; overlying water head ≈ 4 cm; sediment depth ≈ 30 cm) for microsensor measurements were retrieved from the sampling site and incubated not longer than 4 d with in situ water in an aquarium in the laboratory at room temperature (~ 22°C). Amperometric microsensors for NO, N_2O, and O_2 and potentiometric liquid ion exchange microsensors for NO_3^-, NO_2^-, and NH_4^+ were prepared and calibrated as described previously (Schreiber et al. 2008, 2009, and references therein). Vertical

concentration profiles were measured as described previously (Schreiber et al. 2009). The measurements in the cores were done outside the aquarium under dark conditions at room temperature with a moist air jet directed onto the water surface to induce constant flow. Up to three sensors were used simultaneously with their tips adjusted manually to the sediment surface using a dissection microscope (Stemi SV 6; Carl Zeiss AG). The sensor tips were horizontally 1–2 cm apart from each other. Multiple independent profiles were measured for each solute in multiple cores from multiple sampling days (except for NH_4^+ profiles, where all cores were sampled on the same day). The profiles were in steady state, since the repeated measurement of profiles at one location typically gave identical results (data not shown).

Local conversion rates of solutes were calculated from the curvature of steady-state concentration profiles and the molecular diffusion coefficient, D, using a diffusion-reaction model (Gieseke and de Beer 2004). Values used for D were 2.34×10^{-9} m^2 s^{-1} for O_2, 1.98×10^{-9} m^2 s^{-1} for NH_4^+, 1.86×10^{-9} m^2 s^{-1} for NO_2^-, 1.92×10^{-9} m^2 s^{-1} for NO_3^-, 2.36×10^{-9} m^2 s^{-1} for N_2O, and 2.21×10^{-9} m^2 s^{-1} for NO (for references, see Schreiber et al. 2009). The corresponding effective diffusion coefficients in the sediment, D_{eff}, were calculated by multiplying D with the squared porosity: $D_{eff} = D \times \Phi^2$. The presented rates were averaged over 1 mm depth intervals.

Percolation experiments—For percolation experiments, the intact sediment cores were equipped with a valve in the bottom rubber stopper. Percolation was done with either oxic Weser water without supplements or with oxic Weser water supplemented with the chemical NO donor S-nitroso-N-acetylpenicillamine (SNAP; Calbiochem). For the latter experiment, a known volume of water overlying the sediment core was mixed with a stock solution of SNAP to reach a final concentration of 458 μmol L^{-1}. A syringe, connected to the valve, was used to carefully percolate $\sim$ 45 mL (equivalent to a depth of $\sim$ 4.7 cm sediment column) of the overlying, SNAP-containing water within 1–2 min through the core. The water volume drawn into the sediment was replaced by the addition of fresh, SNAP-containing Weser water to the overlying water. Thereafter, repeated vertical microprofiles were measured at different sediment spots to follow the concentration changes of NO, N_2O, and O_2 within the sediment over time. The experiment was replicated three times using cores sampled on different days, which showed identical patterns in their response to SNAP percolation.

SNAP is routinely used in cell biology and mammalian physiology to study the effects of continuous exposure to NO and was applied for the first time in aquatic biogeochemistry in this study. One NO molecule is released per SNAP molecule. The half-life of SNAP reported by the supplier (Calbiochem) is 10 h, but it is dependent on temperature and the medium. We determined the initial NO production rate of 458 μmol L^{-1} SNAP in anoxic Weser water to be 1.1 μmol L^{-1} min^{-1} (66 nmol cm^{-3} h^{-1}), which corresponds to a half-life of $\sim$ 5 h.

Stable isotope incubations—To understand the mechanism of NO consumption in sediments, we incubated Weser sediments with the chemical NO donor SNAP. Unlabeled SNAP (^{14}NO-SNAP) was purchased (Calbiochem), while ^{15}N-labeled SNAP (^{15}NO-SNAP) was prepared from N-acetylpenicillamine (Sigma) and $Na^{15}NO_2$ (Sigma) according to a protocol for the chemical synthesis of SNAP (Chipinda and Simoyi 2006). We determined the half-life of SNAP to be $\sim$ 5 h (*see* section above) and supplied 63 μmol L^{-1} SNAP in the incubation experiments. Based on these two parameters, we calculated an initial NO production rate of SNAP of 7.8 μmol L^{-1} h^{-1}. Thus, SNAP supplied NO for more than 8 h of incubation. The NO production rate of SNAP is in the same range as the maximum NO production rate measured in the sediment (3 μmol L^{-3} h^{-1}; *see* Results section "Transient NO turnover").

The sediment for stable isotope incubations was sampled at the study site with five core liners. Sediment from the depth horizon between 0.5 and 1.5 cm was pooled and mixed at a 1 : 1 ratio with artificial freshwater medium (AF-medium; the composition of the medium is given in Schreiber et al. [2009]) without any inorganic nitrogen and stored overnight at 4°C. On the following day, the overlying water was discarded, and the sediment was washed again with AF-medium. Approximately 2 mL aliquots of wet sediment were transferred into 6 mL exetainers (Labco), and the weight was measured (4.3–4.9 g sediment per exetainer). Each exetainer was filled with 3 mL of AF-medium. The sediment slurries were purged with He for at least 20 min. The closed exetainer was filled up with anoxic He-purged AF-medium, leaving no air bubbles inside. The experimental incubation was started by adding ^{15}N-tracers from anoxic stock solutions to 15 exetainers per ^{15}N-tracer combination. The tracer combinations were: (1) 50 μmol L^{-1} $Na^{15}NO_2$; (2) 63 μmol L^{-1} ^{15}NO-SNAP; (3) 50 μmol L^{-1} $Na^{15}NO_2$ plus 63 μmol L^{-1} ^{14}NO-SNAP; and (4) 63 μmol L^{-1} ^{15}NO-SNAP plus 500 μmol L^{-1} $Na^{14}NO_2$. The sediment slurries in the exetainers were incubated under constant rotation at 25°C. At each of five time points, the incubation was stopped in three replicate exetainers per tracer combination by adding 100 μL of saturated $Hg(II)Cl_2$ solution.

For measuring the concentrations of $^{14,15}N_2$, $^{15,15}N_2$, $^{14,15}N_2O$, and $^{15,15}N_2O$ in the sediment slurries, a He headspace (1.5 mL) was introduced into the exetainers. The headspace was equilibrated with the sediment slurry by vigorous shaking. The masses 28, 29, 30, 44, 45, and 46 were measured in the headspace gas with a multi-isotope mass spectrometer (GAM 200, IP Instruments). The inlet of the mass spectrometer was equipped with a needle that was inserted into the headspace of the exetainer by puncturing its septum. The vacuum line of the mass spectrometer was used to transport the headspace gas into the mass spectrometer together with a He-trickling stream. The gas stream was passed through a cold trap (−20°C, salt-saturated ice-water) to prevent water vapor from entering the mass spectrometer. The gas volume taken from the exetainer was replaced with a dense 10% NaCl solution, which entered the exetainer at the bottom through

a needle. For each sample, 1 mL of gas was withdrawn from the exetainer into the mass spectrometer, which was sufficient to maintain a stable signal of the mass spectrometer for approximately 1 min.

The concentrations of $^{14,15}N_2$ (mass 29), $^{15,15}N_2$ (mass 30), $^{14,15}N_2O$ (mass 45), and $^{15,15}N_2O$ (mass 46) dissolved in the sediment slurries were calculated from the excess of their respective masses over unlabeled standards and from the solubility of the standards. The standard for N_2 was air-saturated water, and the N_2O standard was a 1 mmol L^{-1} N_2O stock solution. To ensure the same partitioning of N_2 and N_2O between the liquid and gas phases in standards and samples, both were prepared in identical vials, had the same headspace volume, and had the same time for headspace equilibration. Signals of the masses 29 and 30 were corrected for the fractions of isotopically labeled N_2O that correspond to the N_2O decay products N_2^+ and NO^+ in the ion source of the mass spectrometer as described previously (Thomsen et al. 1994), whereby a fraction of $^{15,15}N_2O$ decays to $^{15,15}N_2^+$ (mass 30) and fractions of $^{14,15}N_2O$ decay to $^{14,15}N_2^+$ (mass 29) and $^{14}NO^+$ (mass 30).

The slope of the increase in isotopically labeled N_2 and N_2O over time was used to calculate production rates (nmol cm^{-3} wet sediment h^{-1}). The rates of single-labeled ($^{14,15}N_2$ and $^{14,15}N_2O$) and double-labeled ($^{15,15}N_2$ and $^{15,15}N_2O$) species were investigated with a simple model of random isotope pairing, where the production rate of a single-labeled species, R_{single}, can be predicted from the measured production rate of the double-labeled species, R_{double}, with the formula

$$R_{single} = R_{double} \times \left(\frac{2pq}{q^2}\right)$$

where p and q denote the fraction of the total substrate pool (i.e., NO_2^- plus NO) that is ^{14}N-labeled and ^{15}N-labeled, respectively.

Results

Steady-state NO turnover—We measured steady-state microprofiles of NO, O_2, NO_3^-, NO_2^-, N_2O, and NH_4^+ to determine how NO concentrations are related to the conversion activities of other N-cycle processes within permeable river sediment (Fig. 2). Net NO formation was highest in the oxic zone between 0 to 1 mm below the sediment surface, where NO reached a peak concentration of 0.13 μmol L^{-1} (Fig. 2A). We calculated a net NO production rate of 0.11 nmol cm^{-3} wet sediment h^{-1} from the steady-state concentration profiles (Fig. 2D). A distinct layer of N_2O formation could not be detected, i.e., N_2O concentrations were below the detection limit of 1 μmol L^{-1} (Fig. 2C). The apparent decrease of N_2O below the sediment surface might be due to a slight cross-sensitivity of the N_2O sensor with light or O_2.

NO production overlapped with NH_4^+ oxidation between 0 to 1 mm below the sediment surface (Fig. 2D,F). In the upper 1 mm below the sediment surface, the net NO production rate was 0.11 nmol cm^{-3} wet sediment h^{-1}, and the net NH_4^+ consumption rate was 2.2 nmol cm^{-3} wet sediment h^{-1}, while net NO_3^- reduction was absent. Net NO consumption was observed between 2 and 3 mm below the sediment surface, where low O_2 concentrations (between 15 and 50 μmol L^{-1}) coincided with a peak in net NH_4^+ oxidation (10 nmol cm^{-3} wet sediment h^{-1}) and net NO_3^- consumption (22 nmol cm^{-3} wet sediment h^{-1}; Fig. 2A,D–F).

Transient NO turnover—To further investigate NO production in the upper 1 mm, we fixed the position of the NO microsensor at the NO concentration peak, percolated the overlying water through the sediment core, and measured the kinetics of NO re-formation. Percolation of the overlying water led to an immediate disappearance of NO (Fig. 3). However, the NO concentration quickly reestablished (3–4 min) to its initial level. The time to reestablish the steady-state NO concentration was similar between consecutive percolation events (3–4 min). We used the time course data of NO re-formation to calculate the initial rate of NO production (3 μmol L^{-1} pore water h^{-1} or 1.26 nmol cm^{-3} wet sediment h^{-1} at $\Phi = 0.42$). This rate is 12 times higher than the net NO production rate (0.11 nmol cm^{-3} wet sediment h^{-1}) and is about half of the net NH_4^+ oxidation rate (2.2 nmol cm^{-3} wet sediment h^{-1}; Fig. 2F) in this layer as calculated from the steady-state profiles.

To investigate NO consumption in the sediment core, we percolated the chemical NO donor SNAP (458 μmol L^{-1}) into the sediment and measured NO, N_2O, and O_2 profiles repeatedly at 0.1, 2.1, and 20.6 h after percolation (Fig. 4). NO was consumed in the upper sediment layer (0–4 mm) and did not accumulate much above its steady-state concentration (i.e., 0.13 μmol L^{-1}; Fig. 4A), while NO accumulated in deeper sediment layers below 5 mm. O_2 was present in the two zones of NO consumption (i.e., 0–4 mm and $>$ 6 mm). However, NO was also consumed anaerobically at 3.5 to 4 mm sediment depth (Fig. 4A,C). N_2O accumulated to 9 μmol L^{-1} after 2 h in the NO consumption zone at the oxic–anoxic interface (2.5–4 mm; Fig. 4A–C). Low O_2 consumption rates in deeper sediment layers as compared to the upper 6 mm lead to an upward diffusion of O_2 from below directly after percolation (Fig. 4C, red symbols), establishing a second oxic–anoxic interface at 6 mm. N_2O accumulated rapidly to 20 μmol L^{-1} at this deep oxic–anoxic interface.

NO consumption pathways elucidated by stable isotope incubations—We incubated river sediment anoxically with different combinations of ^{15}N-labeled NO donor SNAP or $^{15}NO_2^-$ plus unlabeled ^{14}NO-SNAP or $^{14}NO_2^-$ and measured the formation of $^{14,15}N_2$, $^{15,15}N_2$, $^{14,15}N_2O$, and $^{15,15}N_2O$ to elucidate the consumption mechanisms of NO (Fig. 5). The addition of 50 μmol L^{-1} $^{15}NO_2^-$ alone led to the formation of $^{15,15}N_2$, which can be attributed to denitrification (Fig. 5A). Little N_2O was formed during these incubations (Fig. 5B). The $^{15,15}N_2$ production ceased at the end of the incubation, resulting in a final concentration of 23 nmol N_2 cm^{-3} wet sediment. Multiplying this concentration with the wet sediment volume of 2.4 cm^3 supplied in each vial and with two molecules NO_2^- converted per N_2 formed gives the consumption of

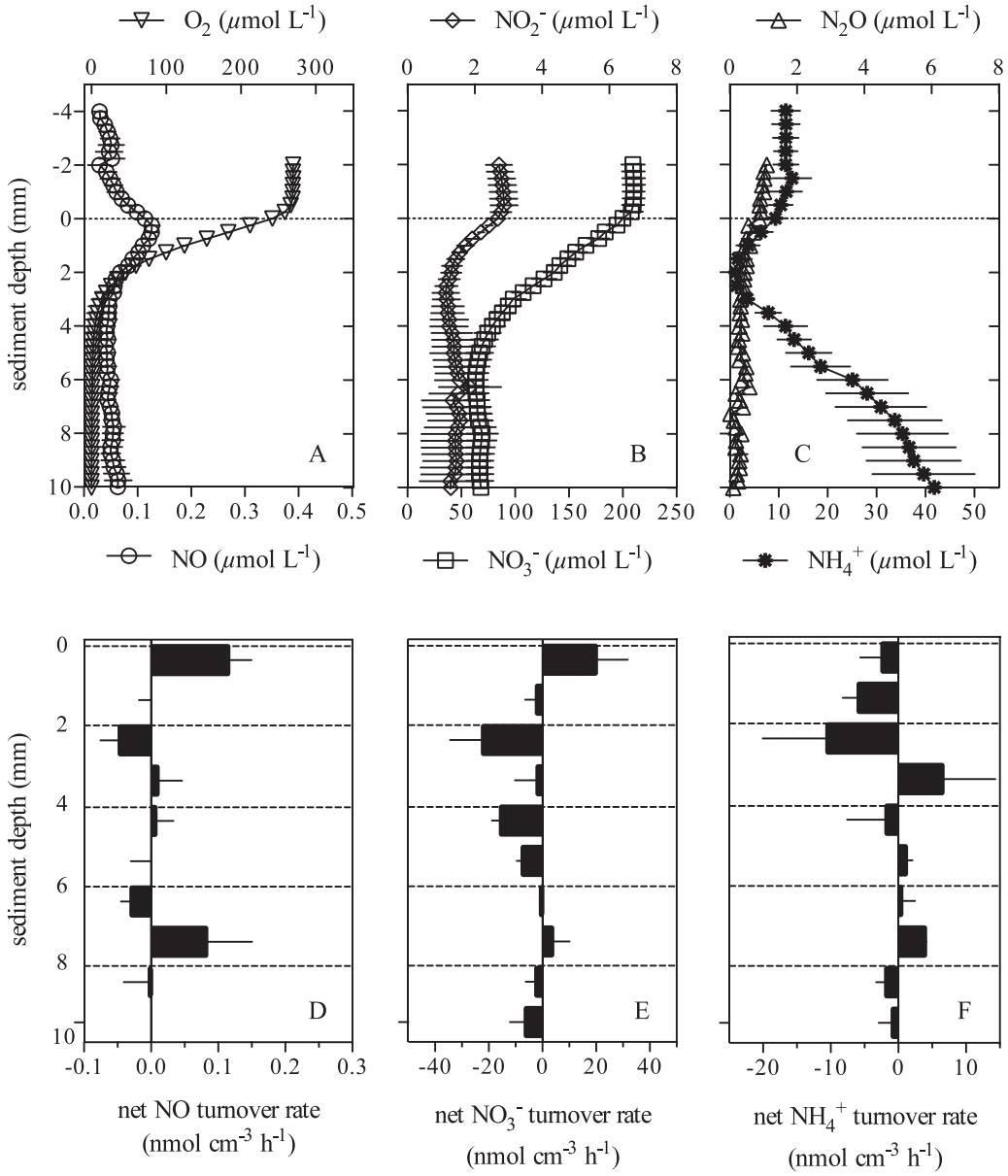

Fig. 2. Biogeochemical context of NO turnover during N-cycling in permeable river sediments (Weser, Germany). (A–C) Pore-water concentrations profiles of (A) NO ($n = 9$), O_2 ($n = 8$), (B) NO_2^- ($n = 4$), NO_3^- ($n = 4$), and (C) NH_4^+ ($n = 3$), N_2O ($n = 4$), measured in sediment cores retrieved from the Weser river. (D–F) Corresponding net volumetric conversion rates of NO, NO_3^-, and NH_4^+ at different sediment depths in nmol cm^{-3} wet sediment h^{-1}, where positive values on the x-scale denote net production, and negative values denote net consumption. On the y-scale, 0 denotes the sediment surface, while positive values denote depth below the sediment surface. The error bars in all panels denote the standard error calculated from multiple independent profiles.

110 nmol NO_2^- (i.e., 18 μmol L^{-1} in 6 mL incubation volume), which is 37% of the supplied $^{15}NO_2^-$ (i.e., 50 μmol L^{-1}). This indicates that denitrification became limited by the presence of e-donor (e.g., reactive organic carbon) in the sediment. The reduction of one molecule NO_2^- to N-N_2 requires three electrons, and 18 μmol L^{-1} NO_2^- could be maximally reduced, implying that the sediment contained reactive organic carbon equivalent to support the one-electron reduction of 54 μmol L^{-1} of an electron acceptor (e.g., NO_2^- reduction to NO or NO reduction to N-N_2O).

The incubations were performed with an artificial freshwater medium free of inorganic nitrogen species to minimize interference by unlabeled inorganic N-compounds. Nonetheless, $^{14,15}N_2$ production was 16% of the total $^{14,15}N_2$ and $^{15,15}N_2$ production (Fig. 5A). Some $^{14}NO_3^-$ or $^{14}NO_2^-$ could have been formed due to the presence of residual O_2 at the beginning of the incubation, allowing AOB to oxidize $^{14}NH_4^+$ released from organic N. If so, about 4 μmol L^{-1} $^{14}NO_2^-$ or $^{14}NO_3^-$ should have been formed based on the rates of $^{14,15}N_2$ and $^{15,15}N_2$ production and assuming random isotope pairing. Alternatively, the

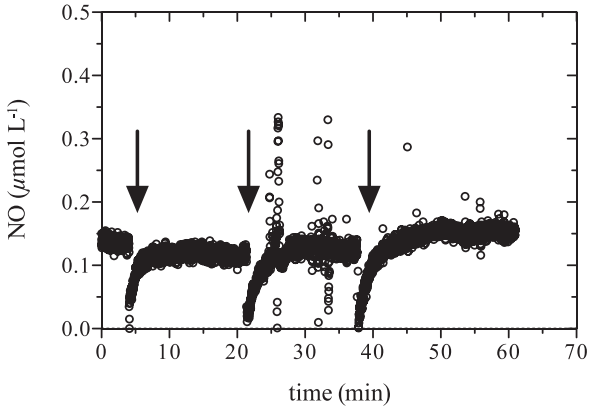

Fig. 3. Transient NO production in permeable river sediments. A NO microsensor was placed in a fixed vertical position within a NO concentration peak at 1 mm depth, and a time series of NO was recorded during repeated percolations of overlying river water into the sediment core at 4 min, 21.4 min, and 37.7 min as indicated by the arrows.

$^{14,15}N_2$ production might have been due to anammox activity, in which case $^{14}NH_4^+$ released from organic N was oxidized with $^{15}NO_2^-$ to $^{14,15}N_2$. The addition of ^{15}NO alone (as 63 μmol L^{-1} ^{15}NO-SNAP) led to the preferential formation of $^{15,15}N_2O$ (23 nmol cm^{-3}) as opposed to $^{15,15}N_2$ (10 nmol cm^{-3}). Thus, N_2O constituted 70% of the total NO converted to N_2 and N_2O in the presence of a continuous NO source (Fig. 5C,D).

Simultaneous addition of 50 μmol L^{-1} of labeled $^{15}NO_2^-$ and unlabeled ^{14}NO (as 63 μmol L^{-1} ^{14}NO-SNAP) led to the preferential formation of N_2O as opposed to N_2 (Fig. 5E,F). Formation of single-labeled $^{14,15}N_2$ and $^{14,15}N_2O$ was higher than double-labeled $^{15,15}N_2$ and $^{15,15}N_2O$ (Fig. 5E,F). The measured rates of $^{15,15}N_2O$ production could explain the rates of single-labeled $^{14,15}N_2O$ production predicted based on random isotope pairing ($R^{calculated}_{14,15N_2O}$ = 1.64 nmol cm^{-3} wet sediment h^{-1} and $R^{measured}_{14,15N_2O}$ = 1.56 nmol cm^{-3} wet sediment h^{-1}).

Incubations with ^{15}NO (as 63 μmol L^{-1} ^{15}NO-SNAP) and a large pool of 500 μmol L^{-1} $^{14}NO_2^-$ again showed that single-labeled $^{14,15}N_2$ and $^{14,15}N_2O$ were preferably produced rather than double-labeled $^{15,15}N_2$ and $^{15,15}N_2O$ (Fig. 5G,H). Moreover, the accumulation of N_2O was higher than that of N_2. Both observations are in agreement with incubations with ^{14}NO plus 50 μmol L^{-1} $^{15}NO_2^-$ (Fig. 5E,F). However, the large NO_2^- pool skewed the random isotope pairing as observed in the incubation with a smaller NO_2^- pool ($^{15}NO_2^-$ and ^{14}NO-SNAP; Fig. 5E,F). The calculated rate of $^{14,15}N_2O$ was approximately two times higher than the measured rate with the large NO_2^- pool ($R^{calculated}_{14,15N_2O}$ = 0.27 nmol cm^{-3} wet sediment h^{-1} and $R^{measured}_{14,15N_2O}$ = 0.12 nmol cm^{-3} wet sediment h^{-1}).

Discussion

Steady-state NO turnover—The novel NO microsensor allowed us to detect distinct biogeochemical features of NO in permeable sediment. NO was produced in the upper 1 mm under oxic conditions, reaching a concentration of 0.13 μmol L^{-1}. The production of NO in the oxic zone, directly below the sediment surface, has also been observed previously with NO microsensors in marine, permeable sediments, where NO reached peak concentrations of 0.5 μmol L^{-1} when measured directly in the field and 0.9 μmol L^{-1} when measured in cores stored for 3 d at 4°C in the laboratory (Schreiber et al. 2008). These previous results from marine sediments indicate that NO measurements in cores might overestimate net NO production occurring in the field, possibly due to an increased flux of

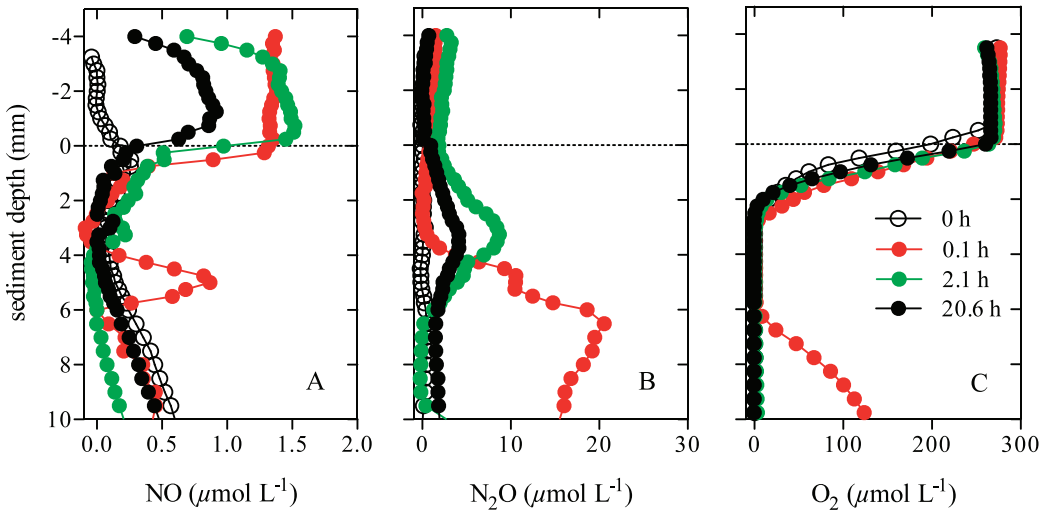

Fig. 4. Microprofiles of (A) NO, (B) N_2O, and (C) O_2 measured before (open symbols) and at intervals of 0.1 h (red), 2.1 h (green), and 20.6 h (black) after the percolation of 45 mL of overlying water containing 458 μmol L^{-1} SNAP (chemical NO donor S-nitroso-N-acetylpenicillamine) into Weser sediment cores. This corresponds to a percolation depth of 47 mm (porosity, Φ = 0.42). On the y-scale, 0 denotes the sediment surface, while positive values denote depth below the sediment surface. We present profiles from a representative experiment, which was replicated three times with cores sampled on different days.

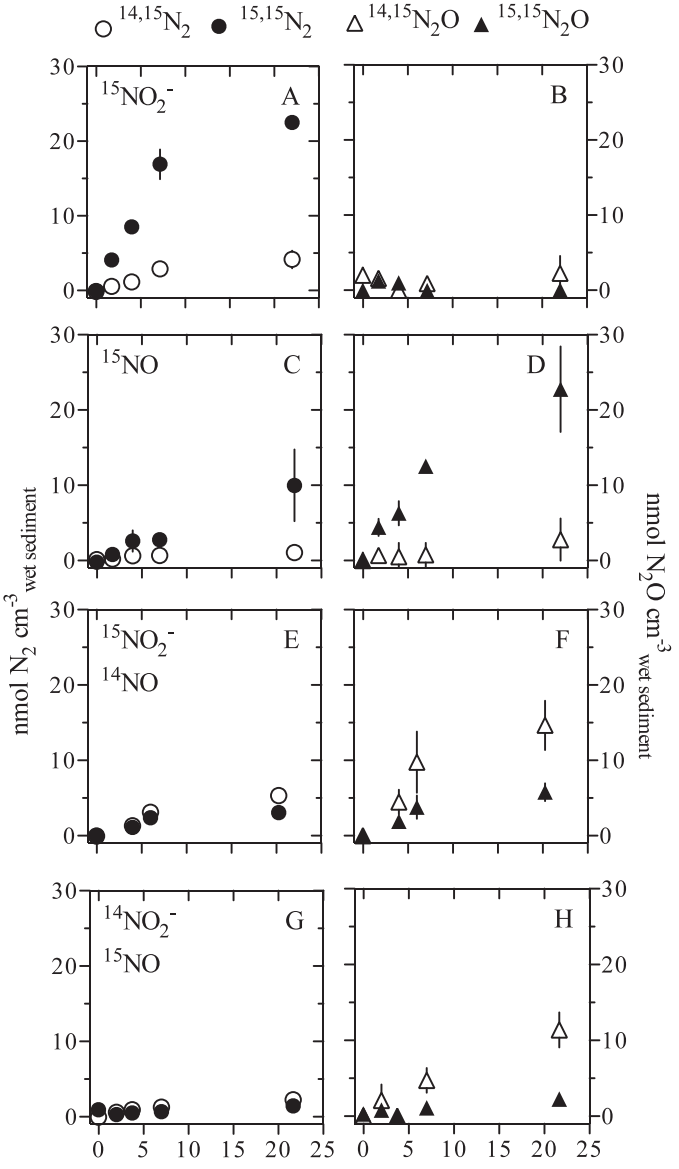

Fig. 5. Anoxic turnover of NO_2^- and NO to N_2O and N_2 in permeable river sediments as assessed by incubation time series with stable nitrogen isotopes. The left panels (A,C,E,G) show the formation of isotopically labeled $^{14,15}N_2$ and $^{15,15}N_2$, and the right panels (B,D,F,H) show the formation of isotopically labeled $^{14,15}N_2O$ and $^{15,15}N_2O$ in nmol cm^{-3} wet sediment. NO was added as the chemical NO donor SNAP (S-nitroso-N-acetylpenicillamine). Separate incubations were performed with He-purged sediment slurries after the addition of (A,B) 50 μmol L^{-1} $^{15}NO_2^-$, (C,D) 63 μmol L^{-1} ^{15}NO-SNAP, (E,F) 50 μmol L^{-1} $^{15}NO_2^-$ plus 63 μmol L^{-1} ^{14}NO-SNAP, and (G,H) 63 μmol L^{-1} ^{15}NO-SNAP plus 500 μmol L^{-1} $^{14}NO_2^-$. The sediment originated from 0.5 to 1.5 cm depth from five cores, and the fresh, pooled samples were washed and mixed with artificial freshwater media, which was depleted of NO_2^- and NH_4^+. The error bars represent the standard deviation of three replicate incubations.

NH_4^+ from deeper sediment strata in static cores as opposed to sediments constantly flushed by advection. A similar overestimation of net NO production rates as opposed to field conditions might have occurred in our core measurements, which should be interpreted as mechanistic experiments rather than field studies.

Our results differ markedly from NO concentration profiles in brackish sediments measured by gas chromatography (Sørensen 1978). NO peaked within or below the denitrification maximum and below the anticipated (O_2 was not measured) oxic zone in these brackish sediments, whereas our measurements showed that NO peaked above the denitrification maximum (Fig. 2A,E) and within the oxic zone. Furthermore, Sørensen (1978) measured NO concentrations up to 200 μmol L^{-1}. Physiological NO concentrations in bacterial cultures measured with an alternative method (NO chemoluminescence) reported free NO concentrations in the nmol L^{-1} range for denitrifiers (Goretski et al. 1990) and nitrifiers (Kampschreur et al. 2008). Furthermore, NO concentrations as high as 200 μmol L^{-1} have been shown to lead to cell death in *Bacillus subtilis* (Moore et al. 2004). Thus, it seems unlikely that the values presented by Sørensen (1978) represent free, dissolved NO. Rather, these high values might be explained by the possible desorption of NO from the sediment during the gas-extraction procedure before the gas chromatographic measurement, as it has been shown that NO can bind to clay particles (Mortland 1965).

NO production overlapped with NH_4^+ oxidation in sediment strata where NO_3^- reduction was absent. This excludes denitrification as a NO-producing pathway and indicates that NO was produced as a by-product of NH_4^+ oxidation in the sediment. Indeed, NO accumulated with a net yield of 0.05 mol NO produced per mol NH_4^+ oxidized at an O_2 concentration of 125 μmol L^{-1} (i.e., 46% air saturation; Fig. 2A,D,F). This implies that, on a net basis, 5% of the oxidized NH_4^+ is lost as NO. It should be noted that we calculated this yield from the net rates that we obtained from steady-state concentration profiles. The gross NO production and gross NH_4^+ consumption might be higher, because of parallel NO consumption and NH_4^+ production within the sediment layer, respectively. Thus, the calculated net NO yield per NH_4^+ oxidized might not reflect the gross NO yield by ammonia oxidizers in the sediment. The net NO yield observed in this study (5% at 46% air saturation or 125 μmol L^{-1} O_2) falls in between previously reported net NO yields in pure cultures (1.2% at 50% air saturation; Kester et al. 1997) and in the oxygen minimum zone (OMZ) of the eastern tropical North Pacific (13% at $O_2 < 100$ μmol L^{-1}; Ward and Zafiriou 1988).

Previous studies showed that nitrifier denitrification by AOB is active under microoxic conditions and is a source for NO formation (Poth and Focht 1985; Kester et al. 1997). In line with this, the highest rates of NO production and NH_4^+ consumption are expected to overlap, and NO production is expected to increase at low O_2 concentration. In contrast, we observed net NO consumption between 2 and 3 mm below the sediment surface, where low O_2 concentrations (between 15 and 50 μmol L^{-1}) coincided with a peak in NH_4^+ oxidation ($\sim$ 10 nmol cm^{-3} wet sediment h^{-1}) and NO_3^- consumption (22 nmol cm^{-3} wet sediment h^{-1}; Fig. 2A,D–F). This observation is consistent with NO measurements in the OMZ of the eastern tropical North Pacific, where peak NO concentrations did not

overlap with the nitrification peak (denitrification was not measured; Ward and Zafiriou 1988). The consumption of NO at low O_2 in the sediments investigated by us can be explained by the parallel occurrence of ammonia-oxidizer–mediated NO formation and denitrification in the same microoxic sediment layer. If NO is indeed reduced by aerobic denitrification at a higher rate than it is produced by NH_4^+ oxidation, then the highest rates of net NO production and NH_4^+ consumption will not overlap, and high NO concentrations will not coincide with low O_2 concentrations. In turn, if high O_2 concentrations directly below the sediment surface between 0 and 1 mm inhibit denitrification as a main NO consumption process, then net NO production can be observed at rather low NH_4^+ oxidation rates and high O_2 concentrations. This explanation for our results is in agreement with studies showing that AOB can produce NO or N_2O as by-products under fully oxic conditions (Shaw et al. 2006; Schreiber et al. 2009) and that aerobic denitrification can occur in permeable sediments (Gao et al. 2010).

In summary, our data indicate that NO is produced as a by-product of NH_4^+ oxidation and accumulates only in the upper oxic sediment layer, because denitrification as a NO consumption process is inhibited there by high O_2 concentrations. A part of this NO is lost to the overlying water by upward diffusion of NO, while the NO that diffuses downward is consumed by denitrification in deeper, microoxic sediment strata, where denitrification is not inhibited anymore by high O_2 concentrations.

Note that our explanation for the spatial dynamics of the NO profile in the oxic sediment zone represents the most plausible interpretation of our results. Experimental proof of this explanation is currently technically not possible, because it is still unclear how gene expression data of N-cycling genes correlate to NO release during the different pathways, and isotope incubations coupled to ^{15}NO measurements are not possible at this high spatial resolution. Furthermore, NO produced by nitrifier denitrification and canonical denitrification cannot be differentiated, and the metabolism of AOB and denitrifiers is coupled via NO_2^-. In addition, NO could chemically react with or adsorb to organic and mineral (e.g., Fe) components of the sediment matrix (Mortland 1965). Testing this hypothesis would require the development of a sterilization method for sediments that does not interfere with NO reactivity, excluding chemical and heat sterilization.

Pure-culture studies have shown that NO is an important regulator for inducing the expression of denitrification genes (Zumft 2002). The NO concentration in the peak (0.13 μmol L^{-1}) is physiologically relevant for NO signaling; e.g., denitrification genes (Nir and Nor) in *Pseudomonas stutzeri* are expressed at 0.05 μmol L^{-1} NO (Zumft 2002 and references therein). Thus, it is conceivable that production of NO by AOB could activate aerobic denitrification. NO can be produced by all catabolic pathways involved in the N-cycle, and it is generally a potent regulatory compound in bacteria. Further studies are needed to investigate the potential of NO in shaping the interactions between N-cycle pathways.

Transient NO turnover—We observed a high initial NO production rate in the upper 1 mm after percolation of overlying water. The initial NO production rate was in the same range as the net NH_4^+ oxidation rate, which supports the interpretation that NO is produced by NH_4^+ oxidation in the upper 1 mm. The result can be explained in two ways. First, the initial rate of NO production represents the *gross* NO production rate (3 μmol L^{-1} h^{-1}). Based on this, the NO turnover time can be calculated by dividing the standing NO concentration of 0.13 μmol L^{-1} by the gross rate. This calculation indicates that the NO pool is turned over within 2.6 min. This means that NO is either a direct intermediate of NH_4^+ oxidation, as has been proposed by Schmidt et al. (2001), or that another "unknown" (chemical or biological) NO production pathway needs to be invoked. The second interpretation is that—in this sediment layer—AOB actively reestablish a preferred steady-state NO concentration by transiently oxidizing most NH_4^+ to NO and not to NO_2^-. In line with this, a pure-culture study showed that a certain extracellular NO concentration is essential for NH_4^+ oxidation activity in *Nitrosomonas eutropha* (Zart et al. 2000).

NO consumption in the sediment was investigated by percolating the chemical NO donor SNAP into the sediment. We observed that layers of NO consumption overlapped with N_2O production and the presence of O_2. The results indicate that NO was reduced to N_2O and support the view that aerobic denitrification is the major driver of NO consumption in the sediment. However, N_2O production could also be facilitated by nitrifier denitrification or NO detoxification with Hmp and NorVW (Gardner et al. 1998, 2002; Kim et al. 1999). Currently, there are no methods to distinguish between these three pathways in sediments.

NO consumption pathways—NO inhibits N_2O reduction: Our data showed that the addition of ^{15}N-labeled chemical NO donor SNAP resulted in the formation of mostly N_2O, while only little N_2 was formed (Fig. 5C–H). The data indicate that N_2O reduction to N_2 is inhibited to a large extent after the addition of SNAP. This is in agreement with biochemical studies on *Pseudomonas perfectomarina* that demonstrated the irreversible inhibition of N_2O reductase (Nos) by NO (Frunzke and Zumft 1986).

We propose two alternative mechanisms for the inhibition of Nos in our experiments. (1) The accumulated N_2O in the incubation vial was not reduced to N_2 toward the end of the incubation, because NO might have inhibited Nos irreversibly. The incubations were done with sediments from 0.5 to 1.5 cm depth. The percolation experiment showed NO accumulation (low NO consumption activity) in the sediment layer below 0.5 cm (Fig. 4A). Possibly, NO accumulation to an inhibitory level for N_2O reduction may have resulted from a higher NO formation rate of the chemical NO donor as compared to the NO consumption rate of the sediment. (2) NO and N_2O reductases compete for electrons, with a preference for Nor as an adaptation to counteract NO accumulation to toxic levels. The e-donor is expended in the incubation vial by the end of the incubation, leaving no electrons to reduce N_2O further to

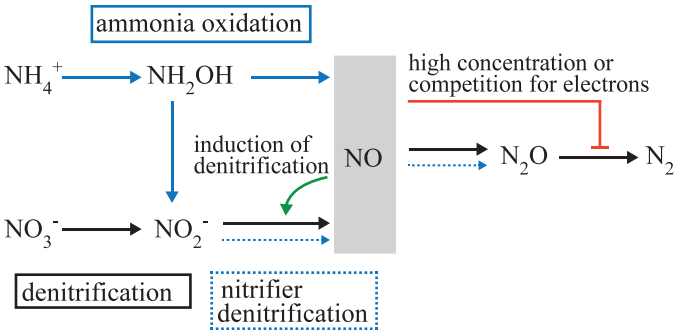

Fig. 6. NO turnover and its effects in sediments. NO can be produced by ammonia oxidation (blue), nitrifier denitrification (blue dashed), and canonical denitrification (black). NO reaches concentrations that are in the range of a signaling molecule for the induction of denitrification (e.g., NO_2^- reduction; green), but this effect remains to be shown in nature. NO forms a common pool (gray box), and its consumption is mediated by denitrification combining one NO molecule derived from NO_2^- with one exogenously supplied NO molecule (potentially supplied by ammonia oxidation or nitrifier denitrification) to form N_2O. The parallel activity of nitrifier denitrification and denitrification cannot be distinguished experimentally and thus potentially contributes to NO consumption. N_2O reduction is inhibited either by high NO concentrations or by competition between NO reduction and N_2O reduction for electrons (red).

N_2. We added 63 μmol L^{-1} of SNAP, donating one molecule NO per molecule SNAP. The incubation with $^{15}NO_2^-$ showed (Fig. 5A) that the sediment only contained reactive organic carbon equivalent to support the one-electron reduction of 54 μmol L^{-1} of an electron acceptor (e.g., NO reduction to N-N_2O). The formation of residual N_2 in the SNAP incubations also supports this second hypothesis, as the complete, irreversible inhibition of N_2O reductases would have not allowed any substantial N_2 formation to occur.

The observation that NO inhibits N_2O reduction is important in order to understand the mechanisms of naturally occurring N_2O accumulation under O_2 fluctuations. Yu et al. (2010) showed that AOB can release high amounts of NO, but not N_2O, upon transition from oxic to anoxic conditions. Our data provide an explanation for the transient accumulation of N_2O upon transition from oxic to anoxic conditions, as has been observed in N-cycling biofilms (Kampschreur et al. 2008; Schreiber et al. 2009) and other ecosystems (discussed in Schreiber et al. 2012): (1) an oxic–anoxic transition leads to NO production by AOB, (2) either high NO concentrations or competition with NO reduction inhibits N_2O reduction, (3) NO is reduced to N_2O, and (4) N_2O accumulates.

NO reduction to N_2O by channeling NO into denitrification: The parallel addition of NO donor and NO_2^- in different ^{15}N-label combinations (Fig. 5E–H) resulted in higher rates of single-labeled $^{14,15}N_2O$ and $^{14,15}N_2$, while addition of ^{15}NO and $^{15}NO_2^-$ alone led to the preferred formation of double-labeled $^{15,15}N_2O$ and $^{15,15}N_2$ (Fig. 5A–D). The results indicate that exogenous NO is channeled into the denitrification pathway, with one endogenous NO molecule from NO_2^- reduction being coupled with one exogenous NO molecule supplied by SNAP. Moreover, combining NO and NO_2^- to form N_2O indicates that NO consumption is coupled to respiration and that exogenous NO is used as an electron acceptor. This supports our explanation for the observed microprofiles measured in the sediment: Aerobic denitrification consumes exogenously supplied NO that is produced by ammonia oxidation.

However, in one treatment, we supplied a large pool of unlabeled $^{14}NO_2^-$ as compared to ^{15}N-labeled chemical NO donor (Fig. 5G,H). In this experiment, the calculated rate of $^{14,15}N_2O$ formation was two times higher than the measured rate based on random isotope pairing. This result indicates that not all exogenously supplied NO molecules are channeled into denitrification by combination with endogenous NO produced from NO_2^- to form N_2O, but that also two exogenous NO molecules could be combined to form N_2O. In addition, the incubation with a large pool of unlabeled $^{14}NO_2^-$ confirms that NO is not oxidized to NO_3^- or NO_2^- for detoxification and subsequently denitrified, because the ^{15}N label would have been trapped in the large pool of unlabeled $^{14}NO_2^-$. Furthermore, the similarity between the results of incubations with different NO_2^- pool sizes (Fig. 5E–H) indicates that there is no or very slow isotopic exchange between NO and NO_2^-. Isotopic exchange would lead to a dilution of ^{15}N label supplied from ^{15}NO-SNAP in the large $^{14}NO_2^-$ pool, resulting in very low accumulation of ^{15}N-labeled N_2O, which was not apparent in our data.

Figure 6 summarizes the findings regarding the turnover of NO in permeable sediment and the possible effects of NO on N-cycling. Our data indicate that NO is produced in the oxic layer by ammonia oxidizers. The NO concentration is in a range where NO potentially acts as a signaling molecule, e.g., for the induction of denitrification genes. The steady-state NO concentration is controlled by ammonia oxidizers, because the removal of NO by percolation results in a reestablishment of the same NO concentration with a rate close to the net NH_4^+ oxidation rate. Denitrification is active in the microoxic sediment layer below the NO peak and consumes NO to undetectable concentrations. Denitrification combines one exogenously supplied NO molecule with one NO molecule generated from NO_2^-. A constant, high supply of NO can lead to the inhibition of N_2O reduction, which might provide a mechanism that explains the transient increase of N_2O concentrations upon O_2 fluctuations. Currently, the understanding of NO and N_2O turnover in complex microbial ecosystems is limited by analytical and molecular techniques. Pathways and the responsible microbes can only be inferred. The present study provides the first measurements and experiments that show a distinct biogeochemical behavior of NO and provide a starting point to further investigate the mechanisms and effects of NO in aquatic sediments and other spatially structured, complex ecosystems.

Acknowledgments

We thank the technical assistants of the Microsensor Research Group at the Max-Planck-Institute for Marine Microbiology in Bremen for preparation of microsensors, the associate editor and

two reviewers for their valuable comments, and the Max Planck Society for financial support.

References

Beaulieu, J. J., and others. 2011. Nitrous oxide emission from denitrification in stream and river networks. Proc. Natl. Acad. Sci. USA **108:** 214–219, doi:10.1073/pnas.1011464108

Beaumont, H. J. E., S. I. Lens, W. N. M. Reijnders, H. V. Westerhoff, and R. J. M. van Spanning. 2004. Expression of nitrite reductase in *Nitrosomonas europaea* involves NsrR, a novel nitrite-sensitive transcription repressor. Mol. Microbiol. **54:** 148–158, doi:10.1111/j.1365-2958.2004.04248.x

Chipinda, I., and R. H. Simoyi. 2006. Formation and stability of a nitric oxide donor: S-nitroso-N-acetylpenicillamine. J. Phys. Chem. B **110:** 5052–5061, doi:10.1021/jp0531107

Corker, H., and R. K. Poole. 2003. Nitric oxide formation by *Escherichia coli*: Dependence on nitrite reductase, the NO-sensing regulator Fnr, and flavohemoglobin Hmp. J. Biol. Chem. **278:** 31584–31592, doi:10.1074/jbc.M303282200

Ettwig, K. F., and others. 2010. Nitrite-driven anaerobic methane oxidation by oxygenic bacteria. Nature **464:** 543–548, doi:10.1038/nature08883

Frunzke, K., and W. Zumft. 1986. Inhibition of nitrous-oxide respiration by nitric oxide in the denitrifying bacterium *Pseudomonas perfectomarina*. Biochim. Biophys. Acta **852:** 119–125, doi:10.1016/0005-2728(86)90064-2

Gao, H., and others. 2010. Aerobic denitrification in permeable Wadden Sea sediments. ISME J. **4:** 417–426, doi:10.1038/ismej.2009.127

Gardner, A. M., R. A. Helmick, and P. R. Gardner. 2002. Flavorubredoxin, an inducible catalyst for nitric oxide reduction and detoxification in *Escherichia coli*. J. Biol. Chem. **277:** 8172–8177, doi:10.1074/jbc.M110471200

Gardner, P. R., A. M. Gardner, L. A. Martin, and A. L. Salzman. 1998. Nitric oxide dioxygenase: An enzymic function for flavohemoglobin. Proc. Natl. Acad. Sci. USA **95:** 10378–10383, doi:10.1073/pnas.95.18.10378

Gieseke, A., and D. de Beer. 2004. Use of microelectrodes to measure in situ microbial activities in biofilms, sediments, and microbial mats, p. 1–23. *In* G. Kowalchuk, F. De Bruijn, I. Head, A. Akkermans, and J. Van Elsas [eds.], Molecular microbial ecology manual. Springer.

Gilberthorpe, N. J., and R. K. Poole. 2008. Nitric oxide homeostasis in *Salmonella typhimurium*: Roles of respiratory nitrate reductase and flavohemoglobin. J. Biol. Chem. **283:** 11146–11154, doi:10.1074/jbc.M708019200

Goretski, J., O. C. Zafiriou, and T. C. Hollocher. 1990. Steady-state nitric oxide concentrations during denitrification. J. Biol. Chem. **265:** 11535–11538.

Hooper, A. B., and K. R. Terry. 1979. Hydroxylamine oxidoreductase of *Nitrosomonas*: Production of nitric oxide from hydroxylamine. Biochim. Biophys. Acta **571:** 12–20, doi:10.1016/0005-2744(79)90220-1

Kampschreur, M. J., N. C. G. Tan, R. Kleerebezem, C. Picioreanu, M. S. M. Jetten, and M. C. M. van Loosdrecht. 2008. Effect of dynamic process conditions on nitrogen oxides emission from a nitrifying culture. Environ. Sci. Technol. **42:** 429–435, doi:10.1021/es071667p

Kartal, B., and others. 2011. Molecular mechanism of anaerobic ammonium oxidation. Nature **479:** 127–130, doi:10.1038/nature10453

Kester, R. A., W. de Boer, and H. J. Laanbroek. 1997. Production of NO and N_2O by pure cultures of nitrifying and denitrifying bacteria during changes in aeration. Appl. Environ. Microbiol. **63:** 3872–3872.

Kim, S. O., Y. Orii, D. Lloyd, M. N. Hughes, and R. K. Poole. 1999. Anoxic function for the *Escherichia coli* flavohaemoglobin (Hmp): Reversible binding of nitric oxide and reduction to nitrous oxide. FEBS Lett. **445:** 389–394, doi:10.1016/S0014-5793(99)00157-X

Meyer, R. L., D. E. Allen, and S. Schmidt. 2008. Nitrification and denitrification as sources of sediment nitrous oxide production: A microsensor approach. Mar. Chem. **110:** 68–76, doi:10.1016/j.marchem.2008.02.004

Moore, C. M., M. M. Nakano, T. Wang, R. W. Ye, and J. D. Helmann. 2004. Response of *Bacillus subtilis* to nitric oxide and the nitrosating agent sodium nitroprusside. J. Bacteriol. **186:** 4655–4664, doi:10.1128/JB.186.14.4655-4664.2004

Mortland, M. M. 1965. Nitric oxide adsorption by clay minerals. Soil Sci. Soc. Am. J. **29:** 514–519, doi:10.2136/sssaj1965.03615995002900050014x

Poth, M., and D. D. Focht. 1985. ^{15}N kinetic analysis of N_2O production by *Nitrosomonas*: An examination of nitrifier denitrification. Appl. Environ. Microbiol. **49:** 1134–1141.

Santoro, A. E., C. Buchwald, M. R. McIlvin, and K. L. Casciotti. 2011. Isotopic signature of N_2O produced by marine ammonia-oxidizing archaea. Science **333:** 1282–1285, doi:10.1126/science.1208239

Schmidt, I., E. Bock, and M. S. Jetten. 2001. Ammonia oxidation by *Nitrosomonas eutropha* with NO_2 as oxidant is not inhibited by acetylene. Microbiology **147:** 2247–2253.

Schreiber, F., B. Loeffler, L. Polerecky, M. M. M. Kuypers, and D. de Beer. 2009. Mechanisms of transient nitric oxide and nitrous oxide production in a complex biofilm. ISME J. **3:** 1301–1313, doi:10.1038/ismej.2009.55

———, L. Polerecky, and D. de Beer. 2008. Nitric oxide microsensor for high spatial resolution measurements in biofilms and sediments. Anal. Chem. **80:** 1152–1158, doi:10.1021/ac071563x

———, P. Wunderlin, K. M. Udert, and G. F. Wells. 2012. Nitric oxide and nitrous oxide turnover in natural and engineered microbial communities: Biological pathways, chemical reactions, and novel technologies. Front. Microbiol **3:** 372, doi:10.3389/fmicb.2012.00372

Shaw, L. J., G. W. Nicol, Z. Smith, J. Fear, J. I. Prosser, and E. M. Baggs. 2006. *Nitrosospira* spp. can produce nitrous oxide via a nitrifier denitrification pathway. Environ. Microbiol. **8:** 214–222, doi:10.1111/j.1462-2920.2005.00882.x

Shen, T., M. Stieglmeier, J. Dai, T. Urich, and C. Schleper. 2013. Responses of the terrestrial ammonia-oxidizing archaeon *Ca. Nitrososphaera viennensis* and the ammonia-oxidizing bacterium *Nitrosospira multiformis* to nitrification inhibitors. FEMS Microbiol. Lett. **344:** 121–129, doi:10.1111/1574-6968.12164

Sørensen, J. 1978. Occurrence of nitric and nitrous oxides in a coastal marine sediment. Appl. Environ. Microbiol. **36:** 809–813.

Stahl, D. A., and J. R. de la Torre. 2012. Physiology and diversity of ammonia-oxidizing archaea. Annu. Rev. Microbiol. **66:** 83–101, doi:10.1146/annurev-micro-092611-150128

Starkenburg, S. R., D. J. Arp, and P. J. Bottomley. 2008. Expression of a putative nitrite reductase and the reversible inhibition of nitrite-dependent respiration by nitric oxide in *Nitrobacter winogradskyi* Nb-255. Environ. Microbiol. **10:** 3036–3042, doi:10.1111/j.1462-2920.2008.01763.x

Thomsen, J. K., T. Geest, and R. P. Cox. 1994. Mass spectrometric studies of the effect of pH on the accumulation of intermediates in denitrification by *Paracoccus denitrificans*. Appl. Environ. Microbiol. **60:** 536–541.

Ward, B. B., and O. C. Zafiriou. 1988. Nitrification and nitric-oxide in the oxygen minimum of the eastern tropical North Pacific. Deep. Res. Part A **35:** 1127–1142, doi:10.1016/0198-0149(88)90005-2

Yu, R., M. J. Kampschreur, M. C. M. van Loosdrecht, and K. Chandran. 2010. Mechanisms and specific directionality of autotrophic nitrous oxide and nitric oxide generation during transient anoxia. Environ. Sci. Technol. **44:** 1313–1319, doi:10.1021/es902794a

Zart, D., I. Schmidt, and E. Bock. 2000. Significance of gaseous NO for ammonia oxidation by *Nitrosomonas eutropha*. Antonie Van Leeuwenhoek **77:** 49–55, doi:10.1023/A:1002077726100

Zumft, W. G. 1997. Cell biology and molecular basis of denitrification. Microbiol. Mol. Biol. Rev. **61:** 533–616.

———. 2002. Nitric oxide signaling and NO dependent transcriptional control in bacterial denitrification by members of the FNR-CRP regulator family. J. Mol. Microbiol. Biotechnol. **4:** 277–286.

Associate editor: Mary I. Scranton

Received: 28 October 2013
Accepted: 14 April 2014
Amended: 16 April 2014